

Gate-tunability of the superconducting state at the EuO/KTaO₃ (111) interface

Weiliang Qiao^{1†}, Yang Ma^{1†}, Jiaojie Yan^{1†}, Wenyu Xing¹, Yunyan Yao¹, Ranran Cai¹, Boning Li¹,
Richen Xiong¹, X. C. Xie^{1,2,3}, Xi Lin^{1,2,3}, Wei Han^{1*}

¹International Center for Quantum Materials, School of Physics, Peking University, Beijing 100871, P. R. China

²CAS Center for Excellence in Topological Quantum Computation, University of Chinese Academy of Sciences, Beijing 100190, P. R. China

³Beijing Academy of Quantum Information Sciences, Beijing 100193, P. R. China

[†]These authors contributed equally to the work

*Correspondence to: weihan@pku.edu.cn

Abstract:

The recent discovery of superconducting interfaces in the KTaO₃ (111)-based heterostructures is intriguing, since a much higher superconducting critical temperature (T_C ; ~ 2 K) is achieved compared to that in the SrTiO₃ heterostructures (~ 300 mK). In this paper, we report the superconducting properties of EuO/KTaO₃ (111) interface as a function of the interface carrier density (n_s). The maximum T_C is observed to be ~ 2 K at $n_s \sim 1 \times 10^{14}$ cm⁻². In addition, we show that the critical current density and the upper critical magnetic field can be effectively tuned by the back gate voltage. Interestingly, the gate dependence of the upper critical magnetic field exhibits a trend opposite to that of T_C in the underdoped region, suggesting a relatively larger Cooper pairing potential.

I. INTRODUCTION

The observation of superconducting interfaces between two insulating oxide layers of SrTiO₃ and LaAlO₃ is fascinating for the field of superconductivity [1-4]. Since then, a lot of efforts has been spent to achieve high temperature superconducting oxide interfaces via the heterostructure engineering and ionic liquid gating, such as LaTiO₃/SrTiO₃ [5], Al₂O₃/SrTiO₃ [6], and KTaO₃ (100) [7], etc. Recently, the superconductivity in KTaO₃ (111)- and KTaO₃ (110)-based heterostructures has been discovered with a superconducting critical temperature (T_C) up to ~ 2.2 K [8-11]. This T_C is much higher than those observed in SrTiO₃ (100)-, SrTiO₃ (111)-, and the KTaO₃ (100)-based heterostructures [1-4,7]. Subsequently, several interesting physical phenomena have been observed, including the anisotropic transport behavior with a possible “stripe”-like phase [8], and the quantum Griffiths transition [9] as well as the electric field control of superconductivity [11]. The pairing mechanism of the superconducting KTaO₃ (111) interfaces poses a theoretical challenge [12]. Experimentally, the systematical investigation of the carrier density (n_s) dependence of various superconducting properties will be necessary for understanding the pairing mechanism of the EuO/KTaO₃ (111) interfaces.

In this paper, we report the superconducting properties of EuO/KTaO₃ (111) interfaces as a function of n_s tuned by varying the EuO growth condition and by applying a back gate on the KTaO₃ crystals. The T_C reaches its maximum of 2 K with $n_s \sim 1 \times 10^{14}$ cm⁻². As n_s varies, the critical current density (J_C) exhibits a trend similar to that of T_C , while the upper critical magnetic field (B_{C2}) exhibits the opposite trend. The opposite trends between B_{C2} and T_C in the underdoped region are similar to the characteristics of high temperature superconducting cuprates, suggesting a relatively stronger Cooper pairing potential at lower n_s . Our results could pave the way for

further understanding of the pairing mechanisms of superconductivity interfaces in the KTaO_3 (111) heterostructures.

II. EXPERIMENTAL

The EuO thin films were grown on the KTaO_3 (111) single crystals via oxide molecular beam epitaxy (MBE-Komponenten GmbH; Octoplus 400) at 500 °C. There were two steps of EuO thin film growth, including the ~ 1 nm Eu thin layer without oxygen and the following ~ 9 nm EuO layer with the oxygen partial pressure of $\sim 1 \times 10^{-9}$ mbar. After the EuO growth, a 5-nm MgO layer was deposited via *e*-beam evaporation *in situ* to protect the EuO films from degradation during subsequent measurements. The EuO/ KTaO_3 Hall bar devices were fabricated using standard photolithography followed by a wet-etching step using diluted hydrochloric acid. The details of the growth conditions and device fabrication process can be found in our previous report [9]. A silver paste was used on the back side of the KTaO_3 crystals to apply the gate voltage (V_g) to tune n_s .

The electron transport properties of EuO/ KTaO_3 heterostructures were measured via either van der Pauw or standard Hall geometries. For T from 300 to 1.5 K, the electrical measurements were conducted in an Oxford Spectromag system with the dc technique ($I_{dc} \sim 100 \mu\text{A}$). The low temperature measurements from $T = 4$ to ~ 0.26 K were performed in a He-3 insert (HelioxVT) in an Oxford TeslatronPT system. In this system, the resistances vs. temperature and magnetic field were measured using a low frequency lock-in technique ($I_{ac} = 1 \text{ nA}$, $f = 17 \text{ Hz}$ or 23 Hz), and the critical current measurements were conducted using a dc source Keithley 2400 and a multimeter Keithley 2000. All the carrier densities were obtained in the Oxford Spectromag system using Hall measurements at $T = 10$ K. The back gate voltage was applied using a Keithley 2400. Gate cycling

was performed prior to the gate-dependence measurement and the normal state R_s shows little change. To be noted, V_g was varied in the range from -200 to 100 V to prevent electric breakdown of the KTaO_3 single crystals under V_g higher than 100 V.

III. RESULTS AND DISCUSSION

Figure 1(a) shows the schematic of the superconducting interfaces between the insulating EuO films and single crystalline KTaO_3 (111) substrates. As described in the experimental section, the interface n_s can be controlled by changing the growth time of EuO in the first step. Generally speaking, the longer growth time of Eu results in higher carrier density for EuO/ KTaO_3 (111) interfaces. The blue, red, black and green curves in Fig. 1(b) show the sheet resistance (R_s) as a function of temperature (T) for four representative samples from #1 to #4. From the zero-resistance temperature, T_C can be identified to be 1.87 K, 1.75 K, 1.33 K and 1.23K for samples #1, #2, #3 and #4, respectively. The results of the onset temperature and uniformity of superconductivity state are shown in the Supplemental Material [13]. The corresponding interfaces n_s are determined to be 1.03×10^{14} , 9.65×10^{13} , 7.97×10^{13} , and $7.74 \times 10^{13} \text{ cm}^{-2}$ via Hall measurement at $T = 10 \text{ K}$. These results indicate the critical role of n_s in T_C , which is consistent with the previous report on the superconducting EuO/ KTaO_3 interface [8].

To further investigate the T_C dependence on n_s , a back gate is applied to finely tune n_s of these as-grown samples, as schematically shown in Fig. 2(a) inset. Firstly, the gate voltage dependence of the sample #1 is studied, and three representative R_s - T curves are shown in Fig. 2(a). Clearly, as V_g varies from -150 to 50 V, the superconducting transitions are almost identical to each other. Figure 2(b) summarizes the results of T_C vs. V_g . Despite the relatively large modulation of n_s (measured at $T = 10 \text{ K}$) as V_g varies (inset of Fig. 2(b)), T_C exhibits little variation. Besides, the R_s -

T_C curves of sample #4 with lower T_C are shown in the Fig. 2(c) measured under V_g from -200 to 100 V. Clearly, the T_C under negative V_g is significantly smaller than the T_C under positive V_g . The V_g dependences of T_C and n_s (measured at $T = 10$ K) are summarized in Fig. 2(d). In general, T_C and n_s show a similar trend as V_g varies between -200 and 50 V. For $V_g > 50$ V, T_C shows a slight decrease as n_s increases from $7.8 \times 10^{13} \text{ cm}^{-2}$ to $8.0 \times 10^{13} \text{ cm}^{-2}$. This discrepancy needs future studies.

Figure 3 shows the summary results of T_C vs. n_s measured on 8 representative samples, where the solid symbols represent the results obtained from the as-grown samples, and hollow circles represent the results obtained under V_g . As n_s increases, T_C first increases, and then saturates with n_s in the range from $\sim 9.5 \times 10^{13}$ to $\sim 1.04 \times 10^{14} \text{ cm}^{-2}$. The results of n_s higher than $\sim 1.04 \times 10^{14} \text{ cm}^{-2}$ cannot be obtained despite a large effort by optimizing the growth conditions and applying V_g . Nevertheless, the saturation of T_C may indicate the superconducting dome feature of the EuO/KTaO₃ interfaces, as illustrated by the dashed line in Fig. 3. This superconducting dome as a function of carrier density is similar to those observed in other two-dimensional superconductors, such as LaAlO₃/SrTiO₃ and MoS₂ [14-17].

Next, we investigate the gate tuning critical current density (J_C) of the superconducting EuO/KTaO₃ (111) interfaces. Figure 4(a) shows three representative current-voltage (I - V) curves measured on the sample #4 at $T = 0.26 \pm 0.01$ K. The critical current (I_C) is obtained to be ~ 2.6 , ~ 10.6 , and $\sim 21.2 \mu\text{A}$ for $V_g = -200$, -100 , and 100 V, respectively. At $V_g = -100$ and 100 V, hysteresis of I - V curves around I_C are observed, which could be attributed to the current heating effect of the superconducting interfaces [18]. At $V_g = -200$ V, I_C decreases significantly compared to that at $V_g = 100$ V, and the hysteresis is no longer observable. Based on the width of the Hall bar device ($W = 100 \mu\text{m}$), J_C is calculated based on $J_C = I_C / W$, and the results of J_C as a function of V_g are shown

in Fig. 4(b). The relationship of J_C vs. V_g follows a trend similar to that of T_C vs. V_g , which is consistent with the previous report at the LaAlO₃/KTaO₃ (111) interface [11]. For sample #1, the critical current density (J_C) exhibits little variation as V_g varies (the data is not shown), which agrees well with the results of T_C vs. V_g (Fig. 2(b)).

In the following, we discuss the gate dependence of B_{C2} . In the previous study [8], different B_{C2} were observed with B perpendicular and parallel to the sample plane, which demonstrates the two-dimensional feature of the superconducting EuO/KTaO₃ (111) interface. In the current work, we focus on the B_{C2} that is perpendicular to the sample plane to investigate the Cooper pairing strength. Figure 5(a) shows the R_s vs. B curves measured at $T = 0.26$ K under various V_g from -100 to 100 V. Clearly, compared to the results at $V_g = -100$ V (red curve), B_{C2} at $V_g = 100$ V (blue curve) decreases significantly.

To quantitatively investigate the relationship between B_{C2} and T_C , we define the upper critical magnetic field ($B_{C2}^{50\%}$) as the field where the resistance is 50% of the normal state resistance, as illustrated by the dashed blue and red arrows in Fig. 5(a). This methodology has been widely used to study B_{C2} in the superconductor research community [19,20]. Clearly, $B_{C2}^{50\%}$ monotonically increases as V_g decreases, as shown in Fig. 5(b), which is opposite to the trend of T_C vs. V_g in the underdoped region. Since B_{C2} is related to the local superconductivity and the coherence length of the Cooper pairs, the opposite trends of $B_{C2}^{50\%}$ and T_C in the underdoped region suggest that the pairing strength of Cooper pairs becomes stronger for lower n_s . This feature of B_{C2} increasing with decreasing n_s (V_g) has been observed previously in several superconducting systems, including the high temperature cuprates, iron-based superconductors, and the LaAlO₃/SrTiO₃ interfaces [15,21,22]. In previous studies, this behavior has been considered as the formation of a “pseudogap” state with local bosonic pairs above T_C [21,23]. The lower T_C with larger pairing

strength can be understood as follows: Since the coherence length (ξ_0) is shorter in the underdoped region ($\xi_0 = \sqrt{\Phi_0/2\pi B_{C2}}$, where Φ_0 is the quantum flux) [24], the bosonic pairs cannot overlap with each other. Together with the dilution of the bosonic pairs at lower n_s , it makes the bosonic pairs harder to condense into a superconducting state, and thus, a lower T_C is observed [22]. Interestingly, the experimental evidences of such “pseudogap” state and the preformation of electron pairs have also been reported in LaAlO₃/SrTiO₃ superconducting interfaces [15,25], indicating that there might be a similar pairing mechanism for the superconducting interfaces between the LaAlO₃/SrTiO₃ and KTaO₃ (111)-based heterostructures.

V. CONCLUSION

In summary, we report gate tunability of the superconducting state of the EuO/KTaO₃ (111) interface and the critical role of n_s in J_C and B_{C2} . The highest T_C obtained is ~ 2 K at $n_s \sim 1 \times 10^{14}$ cm⁻². The opposite trends of B_{C2} and T_C with respect to n_s suggest a stronger Cooper pairing potential and might be the signature of a “pseudogap” state formed in the underdoped region. Our results could pave the way for investigating the pairing mechanisms of the KTaO₃ (111) superconducting interface, and might be helpful for further understanding of superconductivity in low carrier density systems.

ACKNOWLEDGMENTS

This work is supported by the financial support from National Basic Research Programs of China (No. 2019YFA0308401 and No.2017YFA0303301), National Natural Science Foundation

of China (No. 11974025 and 11921005), and the Strategic Priority Research Program of the Chinese Academy of Sciences (No. XDB28000000).

W.Q., Y.M., and J.Y. contributed equally to this work.

References:

- [1] N. Reyren, S. Thiel, A. D. Caviglia, L. F. Kourkoutis, G. Hammerl, C. Richter, C. W. Schneider, T. Kopp, A.-S. Rüetschi, D. Jaccard, M. Gabay, D. A. Muller, J.-M. Triscone, and J. Mannhart, Superconducting Interfaces Between Insulating Oxides. *Science* **317**, 1196 (2007).
- [2] H. Y. Hwang, Y. Iwasa, M. Kawasaki, B. Keimer, N. Nagaosa, and Y. Tokura, Emergent phenomena at oxide interfaces. *Nat. Mater.* **11**, 103 (2012).
- [3] J. Mannhart and D. G. Schlom, Oxide Interfaces—An Opportunity for Electronics. *Science* **327**, 1607 (2010).
- [4] N. Pavlenko, T. Kopp, and J. Mannhart, Emerging magnetism and electronic phase separation at titanate interfaces. *Phys. Rev. B* **88**, 201104 (2013).
- [5] J. Biscaras, N. Bergeal, A. Kushwaha, T. Wolf, A. Rastogi, R. C. Budhani, and J. Lesueur, Two-dimensional superconductivity at a Mott insulator/band insulator interface LaTiO₃/SrTiO₃. *Nat. Commun.* **1**, 89 (2010).
- [6] D. Fuchs, R. Schäfer, A. Sleem, R. Schneider, R. Thelen, and H. v. Löhneysen, Two-dimensional superconductivity between SrTiO₃ and amorphous Al₂O₃. *App. Phys. Lett.* **105**, 092602 (2014).
- [7] K. Ueno, S. Nakamura, H. Shimotani, H. T. Yuan, N. Kimura, T. Nojima, H. Aoki, Y. Iwasa, and M. Kawasaki, Discovery of superconductivity in KTaO₃ by electrostatic carrier doping. *Nat. Nanotechnol.* **6**, 408 (2011).
- [8] C. Liu, X. Yan, D. Jin, Y. Ma, H.-W. Hsiao, Y. Lin, T. M. Bretz-Sullivan, X. Zhou, J. Pearson, B. Fisher, J. S. Jiang, W. Han, J.-M. Zuo, J. Wen, D. D. Fong, J. Sun, H. Zhou, and A. Bhattacharya, Two-dimensional superconductivity and anisotropic transport at KTaO₃ (111) interfaces. *Science* **371**, 716 (2021).
- [9] Y. Ma, J. Niu, W. Xing, Y. Yao, R. Cai, J. Sun, X. C. Xie, X. Lin, and W. Han, Superconductor-Metal Quantum Transition at the EuO/KTaO₃ Interface. *Chin. Phys. Lett.* **37**, 117401 (2020).
- [10] Z. Chen, Z. Liu, Y. Sun, X. Chen, Y. Liu, H. Zhang, H. Li, M. Zhang, S. Hong, T. Ren, C. Zhang, H. Tian, Y. Zhou, J. Sun, and Y. Xie, Two-Dimensional Superconductivity at the LaAlO₃/KTaO₃ (110) Heterointerface. *Phys. Rev. Lett.* **126**, 026802 (2021).

- [11] Z. Chen, Y. Liu, H. Zhang, Z. Liu, H. Tian, Y. Sun, M. Zhang, Y. Zhou, J. Sun, and Y. Xie, Electric field control of superconductivity at the LaAlO₃/KTaO₃ (111) interface. *Science* **372**, 721 (2021).
- [12] D. van der Marel, Tantalates Transcend Titanates. *J. Club Condens. Matter Phys.*(2021),doi: 10.36471/JCCM_May_2021_01.
- [13] See Supplemental Materials at [URL will be inserted by publisher] for onset temperature and uniformity of superconducting state in EuO/KTaO₃ (111) interface.
- [14] A. D. Caviglia, S. Gariglio, N. Reyren, D. Jaccard, T. Schneider, M. Gabay, S. Thiel, G. Hammerl, J. Mannhart, and J. M. Triscone, Electric field control of the LaAlO₃/SrTiO₃ interface ground state. *Nature* **456**, 624 (2008).
- [15] S. C. Shen, B. B. Chen, H. X. Xue, G. Cao, C. J. Li, X. X. Wang, Y. P. Hong, G. P. Guo, R. F. Dou, C. M. Xiong, L. He, and J. C. Nie, Gate dependence of upper critical field in superconducting (110) LaAlO₃/SrTiO₃ interface. *Sci. Rep.* **6**, 28379 (2016).
- [16] J. T. Ye, Y. J. Zhang, R. Akashi, M. S. Bahramy, R. Arita, and Y. Iwasa, Superconducting Dome in a Gate-Tuned Band Insulator. *Science* **338**, 1193 (2012).
- [17] Y. Saito, T. Nojima, and Y. Iwasa, Highly crystalline 2D superconductors. *Nat. Rev. Mater.* **2**, 16094 (2016).
- [18] W. J. Skocpol, M. R. Beasley, and M. Tinkham, Self-heating hotspots in superconducting thin-film microbridges. *J. Appl. Phys.* **45**, 4054 (1974).
- [19] P. Li, F. F. Balakirev, and R. L. Greene, Upper critical field of electron-doped Pr_{2-x}Ce_xCuO_{4-δ} in parallel magnetic fields. *Phys. Rev. B* **75**, 172508 (2007).
- [20] S. I. Vedenev, B. A. Piot, D. K. Maude, and A. V. Sadakov, Temperature dependence of the upper critical field of FeSe single crystals. *Phys. Rev. B* **87**, 134512 (2013).
- [21] Y. Wang, S. Ono, Y. Onose, G. Gu, Y. Ando, Y. Tokura, S. Uchida, and N. P. Ong, Dependence of Upper Critical Field and Pairing Strength on Doping in Cuprates. *Science* **299**, 86 (2003).
- [22] Y. Kohama, Y. Kamihara, S. A. Baily, L. Civale, S. C. Riggs, F. F. Balakirev, T. Atake, M. Jaime, M. Hirano, and H. Hosono, Doping dependence of the upper critical field and Hall resistivity of LaFeAsO_{1-x}F_x (x = 0, 0.025, 0.05, 0.07, 0.11, and 0.14). *Phys. Rev. B* **79**, 144527 (2009).
- [23] T. Timusk and B. Statt, The pseudogap in high-temperature superconductors: an experimental survey. *Rep. Prog. Phys.* **62**, 61 (1999).
- [24] M. Tinkham, *Introduction to superconductivity* (Dover Publications, New York, USA, 2004).
- [25] C. Richter, H. Boschker, W. Dietsche, E. Fillis-Tsirakis, R. Jany, F. Loder, L. F. Kourkoutis, D. A. Muller, J. R. Kirtley, C. W. Schneider, and J. Mannhart, Interface superconductor with gap behaviour like a high-temperature superconductor. *Nature* **502**, 528 (2013).

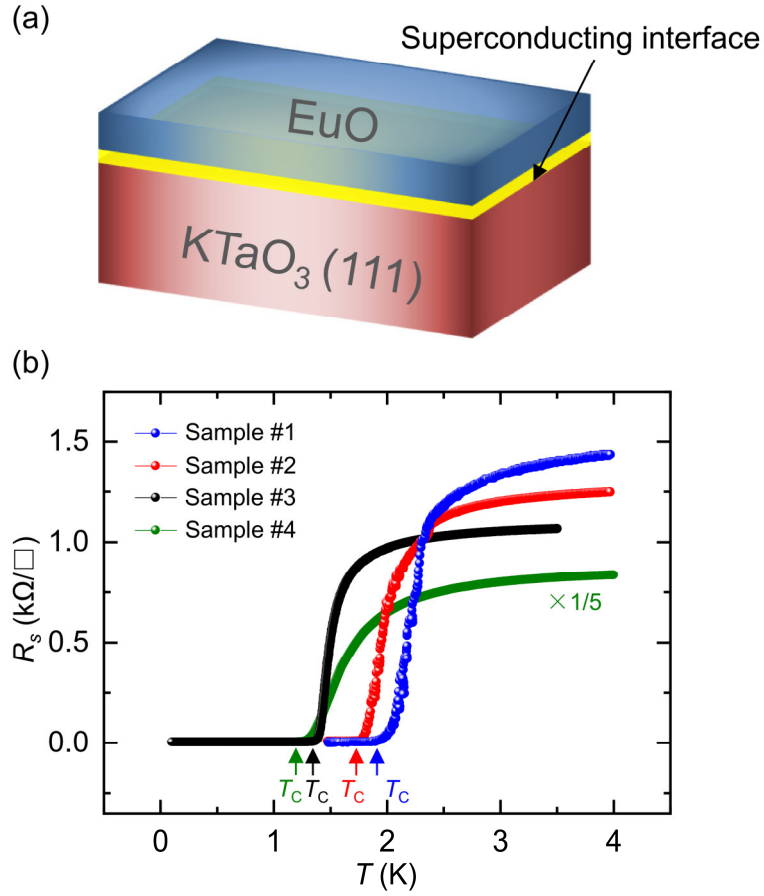


Fig. 1. Schematic and T_C characterization of the superconducting EuO/KTaO₃ (111) interfaces. (a) Schematic of the two-dimensional superconducting interface in EuO/KTaO₃ (111) heterostructures. (b) Temperature dependence of the sheet resistance (R_s) measured on several representative samples with different carrier densities (n_s). T_C is defined as the zero-resistance temperature, as indicated by the arrows. n_s of the sample #1 (blue), #2 (red), #3 (black), and #4 (green) are 1.03×10^{14} , 9.65×10^{13} , 7.97×10^{13} cm⁻², and 7.74×10^{13} cm⁻², respectively, obtained from Hall measurements at $T = 10$ K.

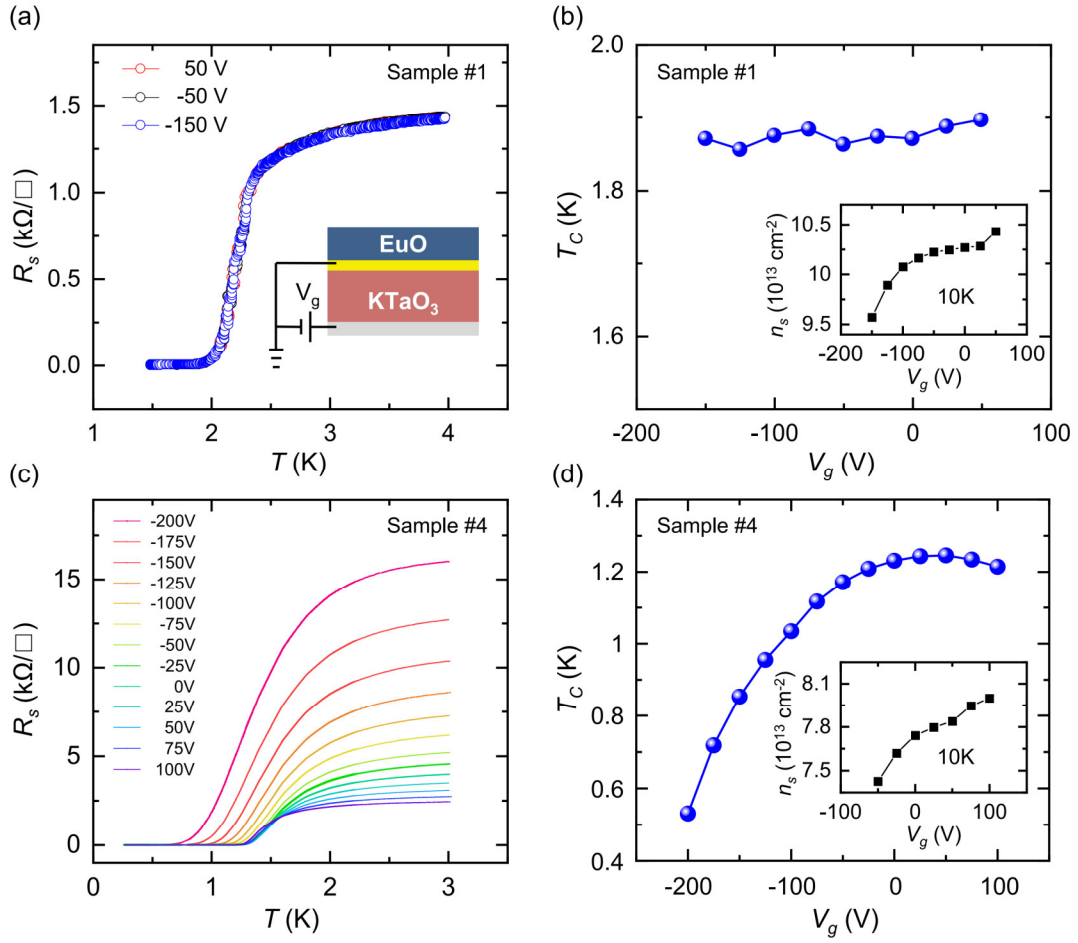


Fig. 2. The gate dependence of T_C of the superconducting EuO/KTaO₃ (111) interfaces. (a) The temperature dependence of R_s of sample #1 at $V_g = -150$, -50 , and 50 V, respectively. Inset: The schematic of the back gate. (b) The gate dependence of T_C of sample #1. Inset: Gate dependence of n_s obtained from Hall measurement at $T = 10$ K. (c) The temperature dependence of R_s of sample #4 under V_g from -200 to 100 V. (d) The gate voltage dependence of T_C of sample #4. Inset: Gate voltage dependence of n_s obtained from Hall measurement at $T = 10$ K. For V_g below -50 V, the Hall probe is no longer good for observing linear Hall resistance to determine the actual n_s .

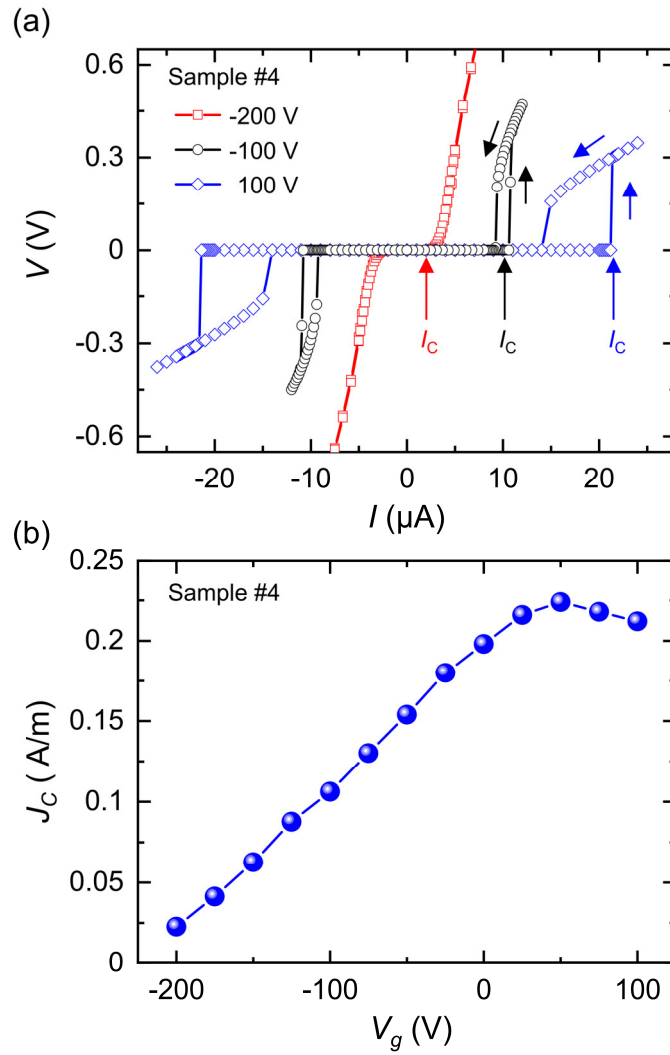


Fig. 4. Gate dependence of the critical current density (J_C) of the EuO/KTaO₃ (111) interface. (a) The current-voltage (I - V) curves of the sample #4 under $V_g = -200$, -100 , and 100 V, respectively. The arrows indicate the critical current (I_C). (b) The gate voltage dependence of J_C of sample #4 which has a similar trend to the $T_C(V_g)$.

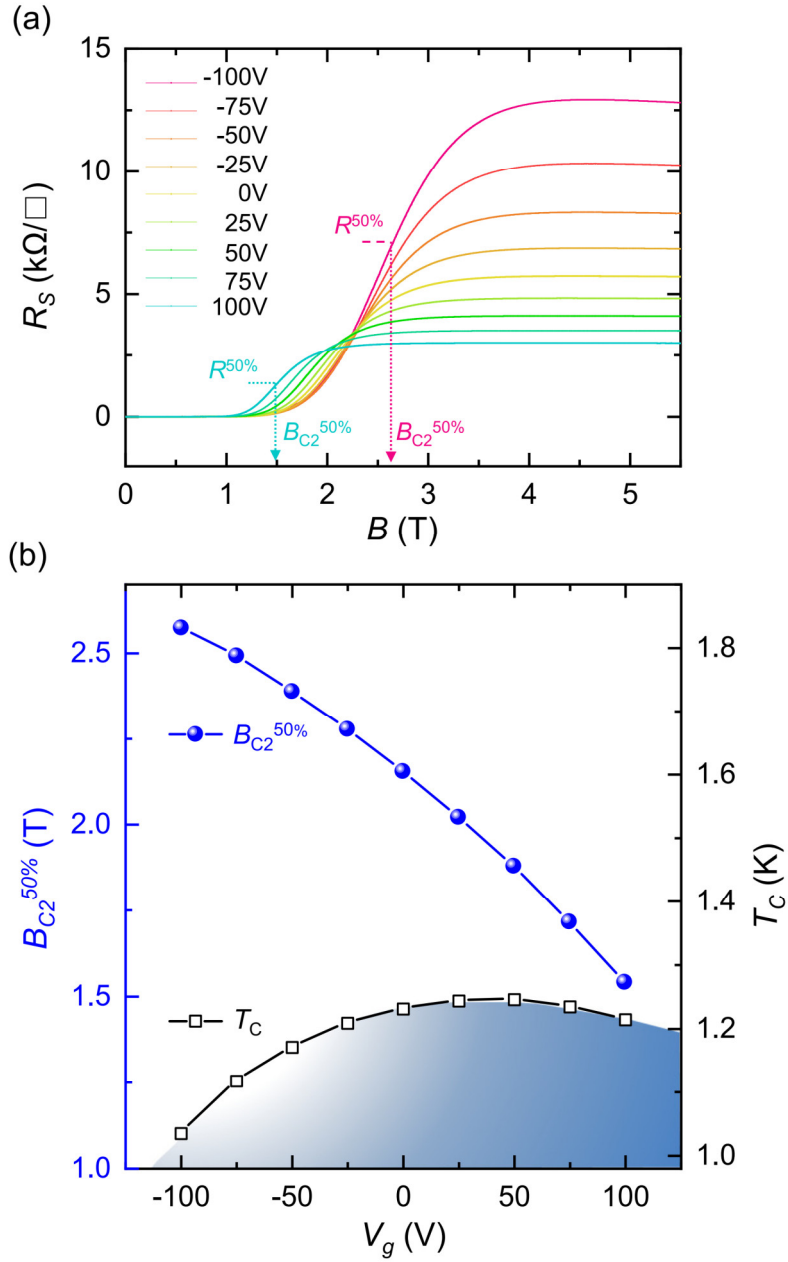


Fig. 5. Gate dependence of the upper critical magnetic field of the EuO/KTaO₃ (111) interface. (a) R_s as a function of magnetic field under V_g from -100 to 100 V obtained on sample #4. For the V_g below -100V, the electrical contacts are no longer good to obtain reliable data under magnetic field. The arrows illustrate the determination of $B_{C2}^{50\%}$, under which R_s is half of its normal state value ($R^{50\%}$) at $V_g = -100$ and 100 V. (b) Gate dependence of $B_{C2}^{50\%}$ and T_c .